Importance of Halide Ions in the Stabilization of Hybrid Sn-Based Coatings for Lithium Electrodes

Arthur Hagopian, Justine Touja, Nicolas Louvain, Lorenzo Stievano, Jean-Sébastien Filhol, Laure Monconduit

Importance of halide ions in the stabilization of hybrid Sn-based coatings for lithium electrodes

Arthur Hagopian,[1,2,§] Justine Touja,[1,§] Nicolas Louvain,[1,2] Lorenzo Stievano,[1,2] Jean-Sébastien Filhol[1,2,*] and Laure Monconduit[1,2,*]

[1] ICGM, Univ Montpellier, CNRS, ENSCM, Montpellier, France

[2] Réseau sur le Stockage Electrochimique de l'Energie (RS2E), FR CNRS 3459, Hub de l'Energie, Amiens, France

[§] A. Hagopian and J. Touja contributed equally to this work.

[*] Corresponding authors: jean-sebastien.filhol@umontpellier.fr, laure.monconduit@umontpellier.fr

Abstract

The properties of hybrid Sn-based artificial SEI layers in protecting Li metal electrode towards surface instabilities were investigated *via* a combined experimental and theoretical approach. The performance of coating layers can be coherently explained based on the nature of the coating species. Notably, when starting from a chloride precursors, the hybrid coating layer is formed by an intimate mixture of Li_7Sn_2 and LiCl: the first ensures a high bulk ionic conductivity, while the second forms an external layer allowing a fast surface diffusion of Li^+ to avoid dendrite growth, a low surface tension to guarantee the thermodynamic stability of the protective layer and a negative underneath plating energy (UPE) promoting lithium plating at the interface between Li metal and the coating layer. The synergy between the two components, and in particular the crucial role of LiCl in the promotion of such an underneath plating mechanism, are shown to be key properties to improve the performance of artificial SEI layers.

1. Introduction

Based on intercalation electrodes, Li-ion batteries (LIBs) seem to have reached their practical limits in terms of energy density. New technologies are therefore needed to face the ever-increasing demand for more powerful energy storage systems. To overcome this challenge, an alternative is to replace the commonly used graphite by lithium metal as negative electrode

material.[1–5] Owing to its low redox potential (-3.04 V *vs.* standard hydrogen electrode) and high theoretical specific capacity (3860 $mAh.g^{-1}$), lithium metal is the perfect candidate to reach higher energy densities than those of LIBs.[6] However, Li-metal batteries (LMBs) are confronted with safety concerns including the growth of whiskers/dendrites which lead to the formation of "dead matter" and ultimately to a short-circuit or thermal runaway of the battery.[6–9] Moreover, the high reactivity of Li generally produces a continuous electrolyte degradation which can cause the battery drying and naturally leads to the formation of an unstable solid electrolyte interphase (SEI) layer on the electrode surface which composition and properties are uncontrolled.[10,11] In order to face these issues, several strategies have been developed including the use of additives in the liquid electrolyte,[12–15] the development of solid electrolytes,[16–19] the development of three-dimensional frameworks[20–22] or the Li metal surface protection with an artificial SEI.[23–26] For the latter, various coating techniques have already been presented to protect the Li metal surface and allow the delay of electrode instabilities, such as atomic layer deposition (ALD), spin coating or direct chemical reaction between a solution and the electrode.[24,27] In this study, we focus on protective layers made by the spontaneous reduction of a metal or semi-metal in contact with lithium to form an intermetallic compound. Nazar's team was the first to propose such a coating by immersing the Li metal in a MCl_x/THF solution (M = In, Zn, Bi and As), to obtain a hybrid layer composed of Li_yM and LiCl as revealed by X-ray diffraction (XRD).[28] Latter on, L. Archer and co-workers introduced an alternative approach to produce a Sn-based coating by depositing a solution of $Sn(TFSI)_2$ in EC/DMC on the Li metal surface.[29] From there on, many artificial coatings have been proposed either based on the use of ionocovalent compounds, most of the time halides, or salts such as $M(TFSI)_x$.[30–37] These studies revealed that, when the metal is introduced in association with a halide, the reaction with Li electrode leads to the formation of a Li-halide by-product often precipitating within the protective layer, whereas when the metal is introduced as a salt, the by-product is a solvated lithium salt. In most cases, the influence of the by-product on the electrochemical performances of the battery is not discussed, and the improvements are generally attributed to the presence of the intermetallic (alloy) compound. Only few studies addressed possible effect of the halide on the coating properties.[28,38,39] It has been highlighted, for instance, that the halide insulating phase is necessary to increase the coating resistivity that reduces electrolyte degradation and lithium plating on the coating surface. Moreover, the electric field gradient that is generated across the coating layer is expected to favour ion transport through the layer and consequently

the plating of lithium underneath the coating layer, which is necessary to maintain the electrode/SEI interface stability over battery cycles.

In fact, although this is not often mentioned in the literature, the artificial SEI should promote such an underneath plating mechanism, which means that Li^+ ions should reduce at the electrode/SEI interface. In general, Li plating can occur 1) at the surface of the coating, 2) within the coating or 3) at the interface between the coating and the electrode.[39] The first case is undesirable because it leads to the formation of fresh lithium oncoming with all its problems (electrolyte degradation, "dead lithium" formation upon oxidation, whisker/dendrite growth, irreversible capacity loss, short cycle life, thermal runaway). The second case does not fulfil either the conditions for a stable artificial coating layer as it leads to the formation of Li nuclei isolated from the electrode inducing an important stress within the coating material which can trigger uneven Li deposition but also the formation of whiskers/dendrites which can potentially break the coating layer. Thus, the only way to achieve a stable Li deposition is to confine it below the artificial coating layer. In some cases, underneath plating revealed by XRD, scanning electron microscopy (SEM), high-resolution transmission electron microscopy (HRTEM), and/or X-ray photoelectron spectroscopy (XPS) analysis have been reached.[28,38–43] Surprisingly, we noticed that such Li underneath plating mechanism is systematically observed when a halide is contained in the protective layer. Unfortunately, in many cases the underneath plating is seldom explained or attributed to the presence of the intermetallic compound regardless of the nature of the by-product formed during the initial chemical reaction. The nature of both M and X in the MX_x coating agent seems to be of importance in order to result in an ideal artificial SEI for Li-metal electrode.

In this work, by introducing the concept of a new thermodynamic driving force for Li to plate underneath the protective layer, further referred as underneath plating energy (UPE), we attempt to demonstrate the halide crucial role in the stability of the plating process. For this purpose, Li electrodes were protected by artificial SEI through a facile ion-exchange reaction with two different solutions: $Sn(TFSI)_2$ or $SnCl_4$ in DME. The nature of the artificial SEI was analysed by XRD and ^{119}Sn Mössbauer spectroscopy. Galvanostatic measurements of symmetric cells associated with density functional theory (DFT) calculations reveals the importance of LiCl phase in such hybrid SEI layers, in order to reach an underneath Li plating. This study also underlines the importance of different properties that an ideal artificial SEI should possess (negative UPE and low surface tension) which, to the best of our knowledge, have not been discussed in detail in the literature so far.

2. Results and discussion

2.1 Fabrication of the hybrid coating and its characterization

To highlight the crucial role of the halide in the artificial SEI, two kinds of coating were prepared by using a 10 mM solution with either $Sn(TFSI)_2$ or $SnCl_4$ mixed with DME. Experimental details are given in Supplementary Information S1. The shiny surface of lithium metal turned black after being in contact with the solution for 30 min, revealing the presence of the artificial coating. Figure 1.a shows the XRD patterns of the two types of materials after the coating process, where the characteristics peaks of Li metal are observed. In $Sn(TFSI)_2$-based coating, only crystalline Sn is detected, whereas that made starting from $SnCl_4$ only leads to crystalline LiCl. Although the formation of Li-Sn alloys is expected, no characteristic peak of Li_xSn is observed by XRD. Since ^{119}Sn Mössbauer spectroscopy is able to detect and identify amorphous Li_xSn compounds, it was used to complement XRD in the investigation of the nature of the coating layer (Figure 1.b). The ^{119}Sn Mössbauer spectrum of the Li-$SnCl_4$ electrode can be fitted with two components with isomer shifts of 1.81 and 2.54 $mm.s^{-1}$, corresponding to Li_7Sn_2 and β-Sn, respectively.[44] In the case of Li-$Sn(TFSI)_2$ electrode, the spectrum fit reveals three spectral components with isomer shifts of 0.00, 1.80 and 2.56 $mm.s^{-1}$, revealing not only the presence of β-Sn and Li_7Sn_2 in the coating layer, but also the formation of traces of SnO_2,[45] possibly coming from the very slight oxidation of the electrode during the measurement.

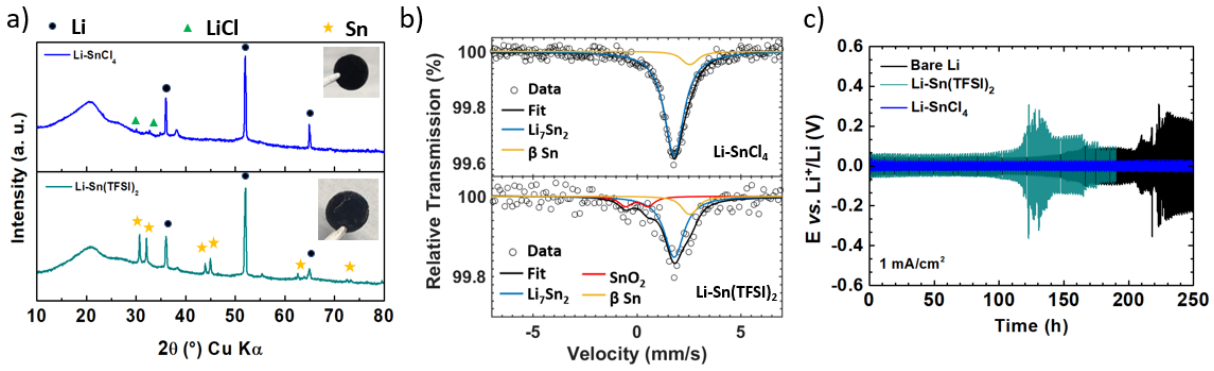

Figure 1: *a) XRD patterns and b) ^{119}Sn Mössbauer spectra of Li-$SnCl_4$ and Li-$Sn(TFSI)_2$ electrodes. c) Galvanostatic measurements of symmetric cells using bare Li, Li-$SnCl_4$ or Li-$Sn(TFSI)_2$ electrodes.*

The Li electrodeposition efficiency of the two coatings was studied in symmetric cells with LiTFSI (1M) in DOL/DME as the electrolyte, and then compared to results obtained with bare Li electrodes (Figure 1.c). The galvanostatic plating/stripping measurements were realised with a current density of 1 $mA.cm^{-1}$ with an areal capacity of 1 $mAh.cm^{-2}$. Although the

polarization of each cell seems very stable at the beginning, around 0.05 V, the overpotential of the Li-$Sn(TFSI)_2$ electrodes becomes chaotic since 100 h of plating/stripping. This anarchic behaviour of the potential can be the consequence of dendrite formation on the electrodes and/or a continuous electrolyte degradation. After 150 h, the same kind of behaviour is observed for the bare Li symmetric cell. The cell made with Li-$SnCl_4$ electrodes shows contrariwise a very stable overpotential at 0.05 V for the whole measurement time of 250 h. The Li plating/stripping seems to be better with these electrodes than with the bare Li or Li-$Sn(TFSI)_2$ electrodes. It is important to note that these results are obtained with only one specific concentration of $SnCl_4$ and $Sn(TFSI)_2$ in the coating solution, and that they can be different with other parameters. Indeed, the layer thickness depends of the concentration and the volume of the deposited solution, which can have an influence on its resistivity and then on the galvanostatic measurements.

During the galvanostatic experiments two plating mechanisms are possible: 1) the lithium is plated at the surface of the artificial SEI layer or 2) the lithium is plated between the artificial SEI layer and the lithium electrode. The poorer performance of the Li plating/stripping with the Li-$Sn(TFSI)_2$ electrodes led us to think that, with this artificial SEI, the plating occurs preferentially on the surface of the SEI layer and the electrode quickly becomes again a "bare Li" electrode. In contrast, the stable polarization measured with Li-$SnCl_4$ electrodes suggests that the Li plating occurs underneath the artificial SEI. In order to verify this hypothesis, the extreme surface (< 10 nm) of the Li-$SnCl_4$ electrodes was studied by XPS before and after cycling (Figure S1). The pristine electrode spectra referred to the XPS data measured for the Li-$SnCl_4$ electrode just after its preparation. The Sn3d and Cl2p spectra confirm the presence of Li-Sn intermetallic compounds as well as LiCl. While no change are noticed on the Li1s, C1s, Sn3d and Cl2p spectra after 2 h of OCV, some peaks appear on the F1s and S2p spectra during the resting time that are due to the presence of typical LiTFSI electrolyte decomposition products.[46] The pristine electrode was never in contact with the electrolyte, explaining why there is no peak on the F1s and S2p spectra for this electrode. After 50 cycles, although the F1s and S2p spectra show the presence of more LiTFSI decomposition compounds, both Li-Sn intermetallic species and LiCl are still detected. It is important to note, however, that a plating of 1 $mAh.cm^{-2}$ is expected to lead to a deposited Li thickness of about 5 µm. [47,48] Therefore, the detection of the artificial SEI compounds by XPS after 50 plating/stripping cycles indicates that the Li^+ ions migrate through the coating layer to

plate underneath. This would explain the better performance of the symmetric cells made with the Li-$SnCl_4$ electrodes.

2.2 Probing Li deposition underneath the artificial coating

In order to probe the Li plating mechanism occurring on the coated metallic electrode, the structural organization of the coating layer has to be properly depicted at the atomic scale. More precisely, the coating surface plays an important role in the plating mechanism as it corresponds to the first site where Li ions may possibly be reduced. Even if the whole coating layer seems to be homogeneous in its bulk (Figure S2), specific surface terminations governed by thermodynamic properties should be preferential. The surface tension and interface tension which can be both computed by DFT calculations can help figuring out the coating structural organization. Details of the calculations are given in Supplementary Information S2. Figure 2.a reveals that the LiCl(100) surface possesses the lower surface tension (7.94 meV.$Å^{-2}$) compared to Li_7Sn_2(100) with any surface termination (30.92, 52.81, 81.64, 111.60 and 167.63 meV.$Å^{-2}$ for Li, $Li_{0.67}Sn_{0.33}$, $Li_{0.5}Sn_{0.5}$, $Li_{0.33}Sn_{0.67}$ and Sn termination, respectively). Even when surfaces are not considered at zero-charge potential but at the experimental one (-0.05V/Li, see Figure 1.c), this hierarchy is conserved (Figure S5). In fact, the electrode potential does not have a significant impact on surface energies as the interfacial capacitance, which is directly related to the curvature of such electro-capillary curves,[6,49–51] is low in glyme solvents. These first results mean that under reasonable kinetic conditions, the coating layer tends to be terminated by LiCl species. This result is also supported by interface tension calculations. The interface between Li electrode and Li_7Sn_2(100) surface terminated by a lithium-rich composition is energetically easier to form than that between Li electrode and LiCl(100) surface. Thus, these results show that 1) the LiCl phase is more stable on the coating surface and 2) the Li_7Sn_2 phase is more stable at the interface with the Li electrode. Henceforth, the presence of chloride in the system would very probably lead to a hybrid coating formed by a layer of Li_7Sn_2 covered by a thin layer of LiCl exposed to the solvent. Thus, any surface property computed on this kind of coating has to be investigated on LiCl surface and not on the intermetallic one.

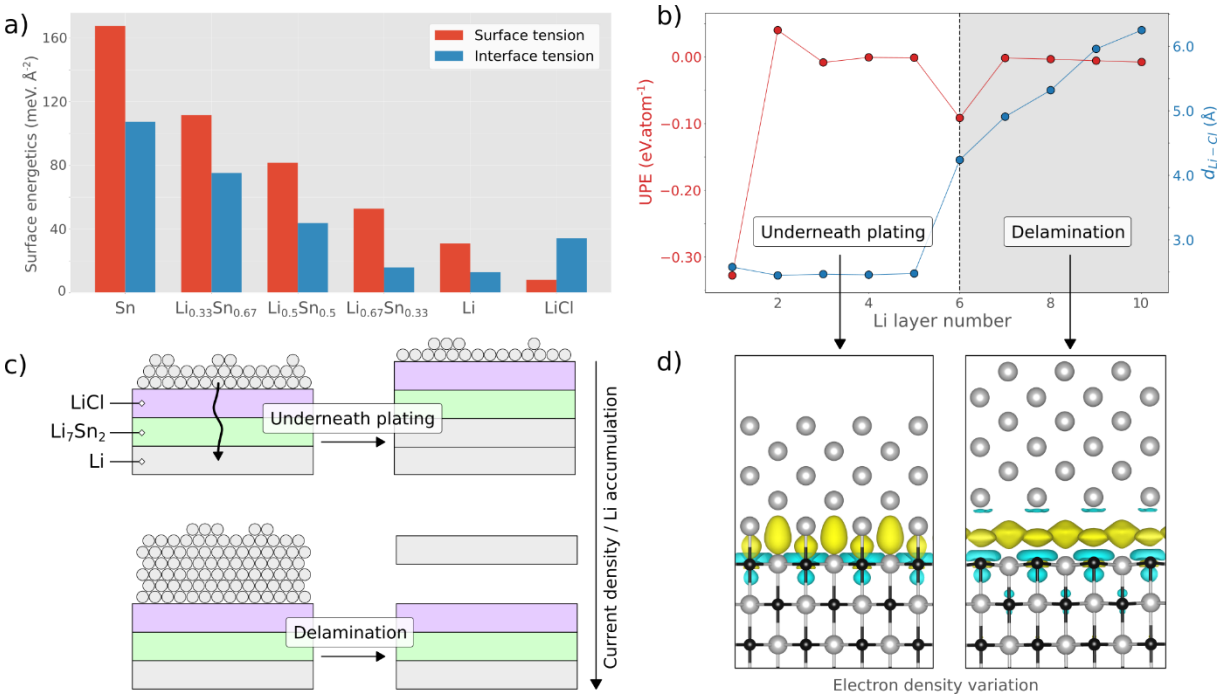

Figure 2: *a) Surface tension (red) and interface tension (blue) of LiCl(100) surface and Li_7Sn_2(100) surface with 5 different surface terminations (Sn, $Li_{0.33}Sn_{0.67}$, $Li_{0.5}Sn_{0.5}$, $Li_{0.67}Sn_{0.33}$, Li). Interfaces correspond to the same six surfaces in contact with a Li(100) surface. b) Underneath plating energy (UPE) and Li-Cl distance for different number of Li layers adsorbed on LiCl(100) surface. c) Schematic representation of underneath plating (top) and delamination process (bottom). d) Electron density variation for 5 (left) and 6 (right) Li adsorbed layers on LiCl(100) surface. Grey and black atoms represent Li and Cl, respectively. Isosurfaces represent the charge variation where yellow and blue correspond to negative and positive regions, respectively.*

In this work, a new thermodynamic driving force for Li to deposit underneath the coating, referred as underneath plating energy (UPE), is introduced. The UPE corresponds to a surface property of the coating and has therefore to be investigated on LiCl surface. The UPE translates the energy cost for an adsorbed Li atom/layer to be plated under the artificial coating (*i.e.* in Li bulk electrode) and, in our case, is defined as

$$UPE = E^s[LiCL] + N.E^b[Li] - E^s[LiCl@N.Li]$$

with $E^s[LiCL]$ and $E^s[LiCl@N.Li]$ corresponding to the LiCl(100) surface energy with and without N adatoms, respectively, and $E^b[Li]$ corresponding to the Li bulk energy. In this case, a negative UPE means that a Li adlayer is more stable on bulk Li than on the coating surface. This first scenario would correspond to a Li deposition underneath the artificial coating and is therefore stable over time. On the contrary, a positive UPE means that the adlayer is more stable on the coating surface. This second scenario would correspond to a Li deposition on the

surface of the artificial coating and is therefore not favorable, as previously discussed. Interestingly, the number of adlayer can be qualitatively related to the current rate as the higher the current density is the most Li atoms are accumulating on the coating surface (the diffusion into the coating layer being limiting compared to the diffusion into the electrolyte). Thus, to highlight the two different deposition regimes (low and high current rate), UPE were computed for one to ten Li adlayers and are shown in Figure 2.b. Except when two adlayers are added on the coating surface, all computed UPE were found negative which means that an underneath plating would be favored on LiCl to any current rate with a metastable state corresponding to two adsorbed Li layers. Nonetheless, a detailed investigation of the structural organization of the system reveals that the interface delaminates when six or more adlayers are added on the coating surface. This is highlighted by the distance measured between a Cl surface atom and an adsorbed Li in the adlayer the closer to the LiCl surface (Figure 2.b). This distance is constant around 2.5 Å from one to five adlayers and increases to more than 4 Å after six adlayers. Thus, two scenarios can arise depending on the applied current density: 1) at low current rate, the Li atoms do not accumulate so much on the coating surface and a stable underneath plating is observed and 2) at high current rate, the coating/adsorbate interface delaminates which is undesirable because it can lead to the formation of dead matter or even dendrites (Figure 2.c). The electron density variation computed for interfaces with and without delamination process can help figuring out the origin of such instability (Figure 2.d). For a large enough layer of Li covering the LiCl surface, the Li layer behaves like a metal and the interface Li atoms are reduced up to the point that the ionic Li^+- Cl^- bond vanishes and a gap opens in between the two phases. This phenomenon is strengthened by the formation of a F center-like region associated with a strong electron transfer in the gap between the very reductive Li surface and the polar LiCl surface inducing a delamination of the two phases. This means that, for too high current densities, when many Li atoms can accumulate on the coating surface, Li metal nuclei can form and dissociate from the surface leading to the formation of "dead matter" in the electrolyte and possibly dendrites.

2.3 What is an ideal artificial SEI

Many works related to artificial SEI focus on a direct control of dendrite formation by the bias of several factors such as surface diffusion,[39,51–54] lithiophilicity[38–40,54–57] and mechanical resistance[39,58] of the coating layer (Figure 3). For instance, a low surface diffusion barrier implies a rapid transport of Li^+ ions on the coating surface, which supports the formation of

smooth surfaces and should help avoiding dendrite growth. A high lithiophilicity (which is directly related to the binding energy of the coating with Li atoms) goes in the same way as it regulates and homogenises Li^+ distribution on the coating surface that favours the formation of smooth surfaces and therefore avoids dendrite growth. Good mechanical resistance should help the electrode to bear volume changes and avoid cracks or delamination which is once again vital to inhibit dendrite growth. All these three factors are necessary for an artificial SEI to be ideal because they guarantee the non-formation of detrimental whiskers/dendrites. Nonetheless, these factors are not sufficient on their own to ensure the stability of the electrode/coating interface over battery cycles as they do not verify 1) that the Li plating process occurs underneath the coating layer, and 2) the thermodynamic stability of the artificial SEI. These two conditions have therefore to be examined through other factors.

An underneath plating mechanism has already been observed for different coating types and the reasons which have been invoked to justify underneath Li deposition are mainly based on the transport kinetic properties of the coating layer. First, Li^+ diffusion into the liquid electrolyte is faster than the diffusion through the solid coating, which corresponds to the limiting step. Thus, a coating material with a high Li bulk diffusivity that do not impede Li-ion diffusion from the electrolyte to the electrode surface is supposed to promote an underneath deposition. J. Qu *et al.* have computed bulk diffusion barriers in tin-based Li-rich intermetallic phases such as Li_7Sn_2 and have shown their high Li diffusivity.[59] Second, the increase in resistance bestowed by an insulating component such as a thin LiCl layer allows establishing a potential gradient across the film which can drive Li^+ ions through the layer.[28] Kinetically speaking, the synergy between a Li conductive alloy and an electronic insulating phase can guarantee a successful underneath plating. In this work, we have introduced the UPE concept, which defines the thermodynamic driving force for Li to plate underneath. For deposition conditions when the Li-kinetics is not limiting, UPE is the main property that allows discriminating a surface plating from an underneath plating mechanism.

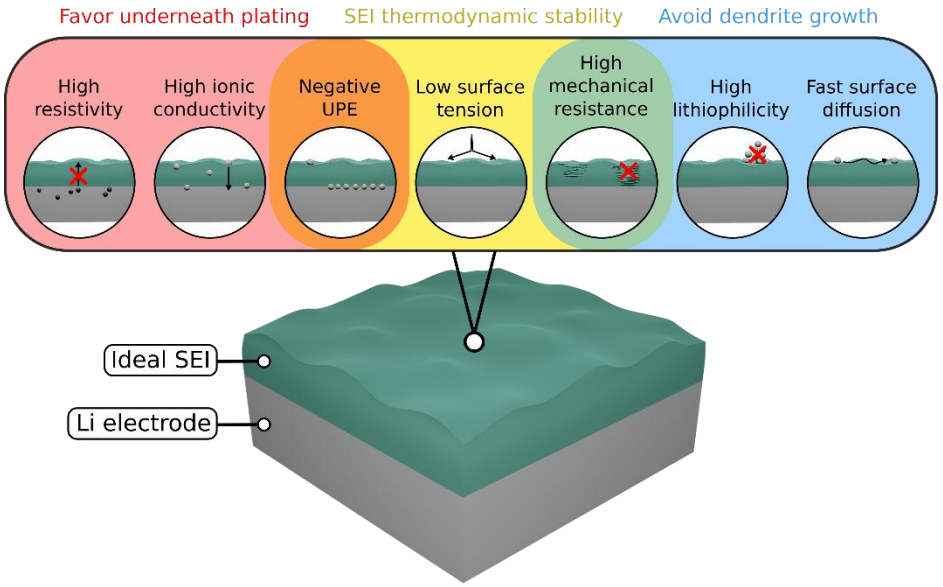

Figure 3: *Schematic illustration of the ideal coating layer properties. These seven properties are regrouped in three categories indicating which feature they impact. An underneath plating is favoured by an artificial SEI with negative UPE, high ionic conductivity and high resistivity. Dendrite growth is avoided by an artificial SEI with high mechanical resistance, high lithiophilicity and fast surface diffusion. The thermodynamic stability of the protective layer is favoured by negative UPE, high mechanical resistance and a low surface tension.*

Finally, the artificial SEI thermodynamic stability over cycling, which is implicitly related to a negative UPE and a good mechanical resistance, is more specifically preserved by a low surface tension. As discussed above, the surface tension dictates which phase is dominant on the coating surface. Thus, if the electrolyte is decomposed during battery cycles, its decomposition products at the interface should not lead to a different surface phase with a lower surface tension than the protective layer one. In such a case, all the surface properties previously set by the artificial SEI layer would be changed and managed by this new surface termination with possibly undesirable properties. Thus, the solvent interface of the coating layer should possess a surface phase with a low surface tension, at least lower than that of a pure Li metal surface, to ensure a stable layer reorganization in the worst scenario where Li^+ ions plate on the coating surface. Li metal surface tensions have been computed by DFT calculations for many surface orientations in implicit solvation conditions and were found to be in the range 29-33 meV.Å^{-2}.[6,51] These values can be reduced to 15-18 meV.Å^{-2} in the presence of explicit carbonate species which correspond to typical ethylene carbonate decomposition products.[6] Consequently, the LiCl(100) surface with a low surface tension of 8

meV.Å^{-2} is once again a good artificial SEI component candidate guaranteeing the thermodynamic stability of the coated electrode surface.

3. Conclusion

In this work, the efficiency of a hybrid Li_7Sn_2/LiCl artificial SEI layer in protecting Li metal electrodes towards surface instabilities is demonstrated experimentally and theoretically. The Li_7Sn_2 component ensures a high bulk ionic conductivity while LiCl forms an external layer and reveals remarkable surface properties: a fast surface diffusion to avoid dendrite growth, a low surface tension to guarantee the thermodynamic stability of the protective layer and a negative UPE to promote an underneath plating mechanism. All the desirable properties to make a coating an ideal SEI were finally gathered to guide future scientific research on the development of artificial SEI layers.

Acknowledgements

The authors thank the French National Research Agency for its financial support through the Labex STORE-EX Labex Project ANR-10LABX-76-01. The "Réseau des Rayons X et Gamma" (Univ. Montpellier, France) is gratefully thanked for granting access to their XRD and Mössbauer spectroscopy platform. Computational work was performed using HPC resources from GENCI-CINES (Grant 2021-A0100910369). The authors would also like to thank Prof. Nobuyuki Zettsu, from Shinshu University, for its contribution on XPS measurements and fruitful discussions. Carine Davoisne (LRCS, UPJV, France) is gratefully thanked for the collection of the SEM images.

References

1. Albertus, P., Babinec, S., Litzelman, S. & Newman, A. Status and challenges in enabling the lithium metal electrode for high-energy and low-cost rechargeable batteries. *Nat Energy* **3**, 16–21 (2018).
2. Hong, H., Che Mohamad, N. A. R., Chae, K., Marques Mota, F. & Kim, D. H. The lithium metal anode in Li–S batteries: challenges and recent progress. *J. Mater. Chem. A* 10.1039.D1TA01091C (2021) doi:10.1039/D1TA01091C.
3. Wang, L. *et al.* Engineering of lithium-metal anodes towards a safe and stable battery. *Energy Storage Materials* **14**, 22–48 (2018).
4. Wang, D. *et al.* Towards High-Safe Lithium Metal Anodes: Suppressing Lithium Dendrites via Tuning Surface Energy. *Adv. Sci.* **4**, 1600168 (2017).
5. Cheng, X.-B., Zhang, R., Zhao, C.-Z. & Zhang, Q. Toward Safe Lithium Metal Anode in Rechargeable Batteries: A Review. *Chem. Rev.* **117**, 10403–10473 (2017).
6. Hagopian, A., Doublet, M.-L. & Filhol, J.-S. Thermodynamic origin of dendrite growth in metal anode batteries. *Energy Environ. Sci.* 10.1039.D0EE02665D (2020) doi:10.1039/D0EE02665D.
7. Liu, Z. *et al.* Dendrite-free Lithium Based on Lessons Learned from Lithium and Magnesium Electrodeposition Morphology Simulations. *Cell Reports Physical Science* **2**, 100294 (2021).
8. Gao, X. *et al.* Thermodynamic Understanding of Li-Dendrite Formation. *Joule* **4**, 1864–1879 (2020).
9. Bai, P., Li, J., Brushett, F. R. & Bazant, M. Z. Transition of lithium growth mechanisms in liquid electrolytes. *Energy Environ. Sci.* **9**, 3221–3229 (2016).
10. Cheng, X.-B. *et al.* A Review of Solid Electrolyte Interphases on Lithium Metal Anode. *Adv. Sci.* **3**, 1500213 (2016).
11. Wang, A., Kadam, S., Li, H., Shi, S. & Qi, Y. Review on modeling of the anode solid electrolyte interphase (SEI) for lithium-ion batteries. *npj Comput Mater* **4**, 15 (2018).

12. Qu, J., Wang, S., Wu, F. & Zhang, C. Effect of Electrolyte Additives on the Cycling Performance of Li Metal and the Kinetic Mechanism Analysis. 11.
13. Piao, N. *et al.* Lithium Metal Batteries Enabled by Synergetic Additives in Commercial Carbonate Electrolytes. *ACS Energy Lett.* 1839–1848 (2021) doi:10.1021/acsenergylett.1c00365.
14. Yang, C.-T., Lin, Y.-X., Li, B., Xiao, X. & Qi, Y. The Bonding Nature and Adhesion of Polyacrylic Acid Coating on Li-Metal for Li Dendrite Prevention. *ACS Appl. Mater. Interfaces* **12**, 51007–51015 (2020).
15. Xu, Y. *et al.* Atomic to Nanoscale Origin of Vinylene Carbonate Enhanced Cycling Stability of Lithium Metal Anode Revealed by Cryo-Transmission Electron Microscopy. *Nano Lett.* **20**, 418–425 (2020).
16. Thangadurai, V., Narayanan, S. & Pinzaru, D. Garnet-type solid-state fast Li ion conductors for Li batteries: critical review. *Chem. Soc. Rev.* **43**, 4714 (2014).
17. Chen, R., Qu, W., Guo, X., Li, L. & Wu, F. The pursuit of solid-state electrolytes for lithium batteries: from comprehensive insight to emerging horizons. *Mater. Horiz.* **3**, 487–516 (2016).
18. Gao, J., Zhao, Y.-S., Shi, S.-Q. & Li, H. Lithium-ion transport in inorganic solid state electrolyte. *Chinese Phys. B* **25**, 018211 (2016).
19. Janek, J. & Zeier, W. G. A solid future for battery development. *Nat Energy* **1**, 16141 (2016).
20. Ni, S., Tan, S., An, Q. & Mai, L. Three dimensional porous frameworks for lithium dendrite suppression. *Journal of Energy Chemistry* **44**, 73–89 (2020).
21. Wang, J. *et al.* Fundamental study on the wetting property of liquid lithium. *Energy Storage Materials* **14**, 345–350 (2018).
22. Zhang, R. *et al.* Conductive Nanostructured Scaffolds Render Low Local Current Density to Inhibit Lithium Dendrite Growth. *Adv. Mater.* **28**, 2155–2162 (2016).
23. Ko, J. & Yoon, Y. S. Recent progress in LiF materials for safe lithium metal anode of rechargeable batteries: Is LiF the key to commercializing Li metal batteries? *Ceramics International* **45**, 30–49 (2019).

24. Xu, R. Artificial Interphases for Highly Stable Lithium Metal Anode. 28 (2019).
25. Qi, L. *et al.* Advances in Artificial Layers for Stable Lithium Metal Anodes. *Chem. Eur. J.* 12 (2020).
26. Liu, W., Liu, P. & Mitlin, D. Review of Emerging Concepts in SEI Analysis and Artificial SEI Membranes for Lithium, Sodium, and Potassium Metal Battery Anodes. *Adv. Energy Mater.* **10**, 2002297 (2020).
27. Touja, J., Louvain, N., Stievano, L., Monconduit, L. & Berthelot, R. An Overview on Protecting Metal Anodes with Alloy-Type Coating. *Batteries & Supercaps* **4**, 1252–1266 (2021).
28. Liang, X. *et al.* A facile surface chemistry route to a stabilized lithium metal anode. *Nat Energy* **2**, 17119 (2017).
29. Tu, Z. *et al.* Fast ion transport at solid–solid interfaces in hybrid battery anodes. *Nat Energy* **3**, 310–316 (2018).
30. Choudhury, S. *et al.* Electroless Formation of Hybrid Lithium Anodes for Fast Interfacial Ion Transport. *Angew. Chem. Int. Ed.* **56**, 13070–13077 (2017).
31. Pang, Q., Liang, X., Kochetkov, I. R., Hartmann, P. & Nazar, L. F. Stabilizing Lithium Plating by a Biphasic Surface Layer Formed In Situ. *Angew. Chem.* **130**, 9943–9946 (2018).
32. Li, F. *et al.* A fluorinated alloy-type interfacial layer enabled by metal fluoride nanoparticle modification for stabilizing Li metal anodes. *Chem. Sci.* **10**, 9735–9739 (2019).
33. Lin, Y., Wen, Z., Yang, C., Zhang, P. & Zhao, J. Strengthening dendrite suppression in lithium metal anode by in-situ construction of Li–Zn alloy layer. *Electrochemistry Communications* **108**, 106565 (2019).
34. Chen, T. *et al.* Dendrite-Free and Stable Lithium Metal Anodes Enabled by an Antimony-Based Lithiophilic Interphase. *Chem. Mater.* **31**, 7565–7573 (2019).
35. Xu, B. *et al.* Engineering interfacial adhesion for high-performance lithium metal anode. *Nano Energy* **67**, 104242 (2020).
36. Liao, K. *et al.* Developing a “Water-Defendable” and “Dendrite-Free” Lithium-Metal Anode Using a Simple and Promising GeCl4 Pretreatment Method. *Adv. Mater.* 8 (2018).

37. Hou, G. *et al.* Facile construction of a hybrid artificial protective layer for stable lithium metal anode. *Chemical Engineering Journal* **391**, 123542 (2020).
38. Whang, G. *et al.* Avoiding dendrite formation by confining lithium deposition underneath Li–Sn coatings. *Journal of Materials Research* (2021) doi:10.1557/s43578-020-00047-8.
39. Hu, A. *et al.* An artificial hybrid interphase for an ultrahigh-rate and practical lithium metal anode. *Energy Environ. Sci.* **14**, 4115–4124 (2021).
40. Zhou, Y. *et al.* A novel dual-protection interface based on gallium-lithium alloy enables dendrite-free lithium metal anodes. *Energy Storage Materials* **39**, 403–411 (2021).
41. Yin, Y.-C. *et al.* Metal chloride perovskite thin film based interfacial layer for shielding lithium metal from liquid electrolyte. *Nat Commun* **11**, 1761 (2020).
42. Lin, L. Lithium phosphide/lithium chloride coating on lithium for advanced lithium metal anode. *Journal of Materials Chemistry A* 9 (2018).
43. Xie, J. *et al.* Stitching h-BN by atomic layer deposition of LiF as a stable interface for lithium metal anode. *Sci. Adv.* **3**, eaao3170 (2017).
44. Robert, F. *et al.* Mössbauer spectra as a “fingerprint” in tin–lithium compounds: Applications to Li-ion batteries. *Journal of Solid State Chemistry* **180**, 339–348 (2007).
45. Nita, C. *et al.* Understanding the Sn Loading Impact on the Performance of Mesoporous Carbon/Sn-Based Nanocomposites in Li-Ion Batteries. *ChemElectroChem* **5**, 3249–3257 (2018).
46. Eshetu, G. G. *et al.* Ultrahigh Performance All Solid-State Lithium Sulfur Batteries: Salt Anion’s Chemistry-Induced Anomalous Synergistic Effect. *J. Am. Chem. Soc.* **140**, 9921–9933 (2018).
47. Chen, S. *et al.* Critical Parameters for Evaluating Coin Cells and Pouch Cells of Rechargeable Li-Metal Batteries. *Joule* **3**, 1094–1105 (2019).
48. Yang, C. *et al.* An Electron/Ion Dual-Conductive Alloy Framework for High-Rate and High-Capacity Solid-State Lithium-Metal Batteries. *Adv. Mater.* **31**, 1804815 (2019).

49. Hagopian, A., Falcone, A., Ben Yahia, M. & Filhol, J.-S. Ab initio modelling of interfacial electrochemical properties: beyond implicit solvation limitations. *J. Phys.: Condens. Matter* **33**, 304001 (2021).
50. Kopač Lautar, A., Hagopian, A. & Filhol, J.-S. Modeling interfacial electrochemistry: concepts and tools. *Phys. Chem. Chem. Phys.* **22**, 10569–10580 (2020).
51. Hagopian, A., Kopač, D., Filhol, J.-S. & Lautar, A. K. Morphology evolution and dendrite growth in Li- and Mg-metal batteries: a potential dependent thermodynamic and kinetic multiscale ab initio study. *Electrochimica Acta* 136493 (2020) doi:10.1016/j.electacta.2020.136493.
52. Jäckle, M. & Groß, A. Microscopic properties of lithium, sodium, and magnesium battery anode materials related to possible dendrite growth. *The Journal of Chemical Physics* **141**, 174710 (2014).
53. Fan, L., Zhuang, H. L., Gao, L., Lu, Y. & Archer, L. A. Regulating Li deposition at artificial solid electrolyte interphases. *J. Mater. Chem. A* **5**, 3483–3492 (2017).
54. Xu, N., Li, L., He, Y., Tong, Y. & Lu, Y. Understanding the molecular mechanism of lithium deposition for practical high-energy lithium-metal batteries. *J. Mater. Chem. A* **8**, 6229–6237 (2020).
55. Yang, D. *et al.* Mechanisms of the Planar Growth of Lithium Metal Enabled by the 2D Lattice Confinement from a $Ti_3C_2T_x$ MXene Intermediate Layer. *Adv. Funct. Mater.* 2010987 (2021) doi:10.1002/adfm.202010987.
56. Chen, Q. *et al.* Li–Zn Overlayer to Facilitate Uniform Lithium Deposition for Lithium Metal Batteries. *ACS Appl. Mater. Interfaces* **13**, 9985–9993 (2021).
57. Luan, J. *et al.* Sn layer decorated copper mesh with superior lithiophilicity for stable lithium metal anode. *Chemical Engineering Journal* **395**, 124922 (2020).
58. Liu, Z. *et al.* Interfacial Study on Solid Electrolyte Interphase at Li Metal Anode: Implication for Li Dendrite Growth. *J. Electrochem. Soc.* **163**, A592–A598 (2016).

59. Qu, J., Xiao, J., Wang, T., Legut, D. & Zhang, Q. High Rate Transfer Mechanism of Lithium Ions in Lithium–Tin and Lithium–Indium Alloys for Lithium Batteries. *J. Phys. Chem. C* **124**, 24644–24652 (2020).